OPTIMAL CONTROL APPLICATIONS & METHODS, VOL. 1, 319–334 (1980)

APPLICATION OF AN ADVANCED TRAJECTORY OPTIMIZATION METHOD TO RAMJET PROPELLED MISSILES

S. W. PARIS
Boeing Aerospace Company, P.O. Box 3999 M/S 8C-05, Seattle, Washington 98128, U.S.A.

B.K. JOOSTEN
NASA Johnson Space Center, Houston, Texas, U.S.A.

AND

L. E. FINK
Boeing Aerospace Company, P.O. Box 3999 M/S 8C-05, Seattle, Washington 98128, U.S.A.

SUMMARY

The mission performance characteristics of ramjet-propelled missiles are highly dependent upon the trajectory flown. Integration of the trajectory profile with the ramjet propulsion system performance characteristics to achieve optimal missile performance is very complex. Past trajectory optimization methods have been extremely problem dependent and require a high degree of familiarity to achieve success. A general computer code (CTOP) has been applied to ramjet-powered missiles to compute open-loop optimal trajectories. CTOP employs Chebyshev polynomial representations of the states and controls. This allows a transformation of the continuous optimal control problem to one of parameter optimization. With this method, the trajectory boundary conditions are always satisfied. State dynamics and path constraints are enforced via penalty functions. The presented results include solutions to minimum fuel-to-climb, minimum-time-to-climb, and minimum time-to-target intercept problems

KEY WORDS Trajectory optimization Ramjet performance Parameter optimization approximation Penalty function methods

INTRODUCTION

The ability of ramjet-powered missiles to perform missions can be greatly enhanced through reliable flight path and performance optimization methods. These methods provide an analytical capability which permits the exploration of missile concepts and their ability to achieve specified performance goals. Techniques to derive optimal solutions to ramjet trajectory problems are extremely difficult, if not impossible, to obtain using most generalized programs due to the highly non-linear behaviour of the propulsion system. The Chebyshev trajectory optimization program (CTOP) has the ability to optimize ramjet missile performance for a variety of problems which include general constraints on the trajectory and missile operating conditions.

This paper presents the CTOP methodology and the results of three trajectory optimization problems for a typical air-to-air, liquid fuel, ramjet-powered missile. These problems are: (1) minimum fuel-to-climb, (2) minimum time-to-climb, and (3) minimum time-to-intercept for both two and three dimensional engagements. No attempt was made to optimize missile design. Such design optimization was emphasized in previous studies.[1, 2]

0143–2087/80/0401–0319$01.00

Received 11 February 1980
Revised 7 May 1980

PROBLEM STATEMENT

The general optimal control problem which we are interested in solving is to obtain the control time histories (i.e. angle of attack, throttle setting), $\mathbf{u}(t)$, which minimize (or maximize) a performance index

$$J = \Phi(\mathbf{x}_f', \mathbf{x}_f, \mathbf{y}_f, t_f) \tag{1}$$

where the state variables $\mathbf{x}$ and $\mathbf{y}$ are subject to the second- and first-order differential equations

$$\begin{aligned} \mathbf{x}'' &= \mathbf{f}(\mathbf{x}', \mathbf{x}, \mathbf{y}, \mathbf{u}, t) \\ \mathbf{y}' &= \mathbf{g}(\mathbf{x}', \mathbf{x}, \mathbf{y}, \mathbf{u}, t) \end{aligned} \tag{2}$$

These equations are typically the equations of motion and the mass flow equation, respectively. The state variables may be subject to non-linear constraints at the initial and final times.

Additionally, path constraints of the form

$$h(\mathbf{x}', \mathbf{x}, \mathbf{y}, \mathbf{u}, t) \leqslant 1 \tag{3}$$

such as angle of attack, load factor, maximum altitude, etc., may also be included. The initial and final times need not be specified.

SOLUTION METHOD

The basic solution technique was first applied to the computation of optimal low-thrust interplanetary transfers.[3, 4] Recently, the method has been applied to atmospheric trajectories[5] and is similar to that described by Balakrishnan.[6] The procedure used is to always satisfy the boundary conditions and then to require the trajectory to satisfy the path and differential (equations of motion) constraints. Convergence of the trajectory to the equations of motion and other constraints while optimizing is accomplished through the use of penalty functions. The performance index is augmented as follows.

$$P^* = J + \frac{1}{\varepsilon}\left\{ \int_{t_i}^{t_f} (\mathbf{x}'' - \mathbf{f})^{\mathrm{T}} \mathbf{W}_x (\mathbf{x}'' - \mathbf{f})\,\mathrm{d}t + \int_{t_i}^{t_f} (\mathbf{y}' - \mathbf{g})^{\mathrm{T}} \mathbf{W}_y (\mathbf{y}' - \mathbf{g})\,\mathrm{d}t + \int_{t_i}^{t_f} \mathbf{V}(h)^{\mathrm{T}} \mathbf{W}_h \mathbf{V}(h)\,\mathrm{d}t \right\} \tag{4}$$

Here $\mathbf{W}_x, \mathbf{W}_y, \mathbf{W}_h$ are diagonal weighting matrices which are chosen to make their particular integral dimensionally invariant. $V(h)$ is defined as

$$V(h) = \begin{cases} 0, & h \leqslant 1 \\ (h-1)^3/B^2 - (h-1)^4/B^3, & 1 < h \leqslant 1+B \\ h-1-B, & h \geqslant 1+B \end{cases} \tag{5}$$

The parameter $B > 0$ allows V to be twice continuously differentiable, and the value $B = 0{\cdot}05$ has been found to be reasonable for the inequality constraints.

The quantity P^* is then minimized for decreasing values of ε. The optimum is reached when P^* is minimized and ε is sufficiently small. In theory, one should be able to pick a sufficiently small value of ε and obtain a single converged solution. In practice, we have found it necessary to solve a sequence of subproblems with decreasing ε since the distortion caused by small values of ε will often cause the numerical minimization of P^* to converge extremely slowly if a solution had not been previously obtained at a more moderate value of ε.

Selection of the initial value of ε is accomplished by means of an adaptive procedure.[5] The procedure finds an initial value of ε which allows constraints to be 'felt' while requiring that the

actual performance index be minimized. After the initial ε is chosen, the subsequent subproblems decrease ε by a fixed fraction (usually $\frac{1}{4}$).

Trajectory representation

To implement the above procedure, it is necessary to have a representation of the complete trajectory. In our program, the state and control variable time histories are represented by Chebyshev polynomials. The polynomial representation allows the differentiation ($\mathbf{x}''$, $\mathbf{x}'$, $\mathbf{y}'$) and integration of equation (4) to be performed in closed form. Rather than choosing the coefficients of the polynomials to satisfy the boundary conditions and the differential and path constraints, we instead use the interpolating properties of the Chebyshev polynomials. Values of the states and controls are chosen at discrete time points, and these values are used to construct the polynomials. The Chebyshev polynomials allow the interpolation to be done in matrix form. Defining a vector $\mathbf{w}$ of a given variable at discrete time points, we can write[3]

$$\mathbf{x}(t) = \mathbf{A}(t)\mathbf{w} \tag{6}$$

Also

$$\mathbf{x}'(t) = \mathbf{A}'(t)\mathbf{w} \tag{7}$$

and

$$\mathbf{x}''(t) = \mathbf{A}''(t)\mathbf{w} \tag{8}$$

By setting the appropriate elements of $\mathbf{w}$ to the initial and final values of $\mathbf{x}$, we are able to fix the boundary conditions for $\mathbf{x}(t)$. Currently, no boundary conditions are imposed on the control variables. Thus, the various boundary conditions can be either variable or fixed without adding any additional terms such as costate or influence variables.

The accuracy of the trajectory representation is governed by the number of points used to construct the interpolating polynomials. Rather than use one high-order polynomial for the entire trajectory, we divide the trajectory into segments called legs and use one polynomial per leg. The polynomials are patched together at each leg juncture. The leg junctions are called patch points. The state variables are required to be continuous and have continuous derivatives across a patch point. No constraints are placed on the control variables at a patch point. By patching polynomials together, the $\mathbf{A}$, $\mathbf{A}'$, and $\mathbf{A}''$ matrices in equations (6)–(8) become banded, which aids in their manipulation. There are several trades that can be made between the order of the polynomials and the number of legs. From experience, it appears that eighth-order polynomials tend to work well. The number of legs which are needed for an accurate solution is problem dependent. Selection of the number of legs is covered in the convergence section of this paper.

Before we solve the optimal control problem, the free elements of the vector $\mathbf{w}$ for each state and control variable are combined into a single array, $\mathbf{z}$. The $\mathbf{z}$ elements are used to minimize the augmented payoff function, P^*. Thus, the variational problem has been converted to one of parameter optimization with the parameters being the elements of $\mathbf{z}$. An added feature of this approach is that the user's initial iterate consists of the elements of $\mathbf{z}$, which are a simple estimate of the controls and trajectory.

Minimization technique

The minimization procedure which is used is a modified Newton iteration. The modified Newton iteration is characterized by using the efficient square root method[7] to solve for the parameter updates. To provide the square root method with a positive-definite matrix, the Hessian is scaled.

The exact workings of the method are given by Hargraves *et al.*[5] This method is a second-order technique which provides both the necessary and sufficient conditions (zero gradient and positive definite Hessian matrix) which proves, at least locally, that an optimum has been reached. We feel that this feature, plus the reduction in the number of iterations, justify the added effort of implementing a second-order optimizer.

Convergence criteria

There are several conditions which must be satisfied before a problem has a converged solution. The subproblems, each for a fixed value of ε, must converge with a near zero gradient and a positive definite Hessian. The performance index for a sequence of subproblems must converge to a single value. The residual errors in the trajectory representation [the integral terms of equation (4)] should approach zero. An indication as to whether or not the residuals are small enough can be obtained by comparing the final states as represented by the polynomials and the final states obtained by numerically integrating the equations of motion using the polynomial representations for the controls. If the residuals do not converge to a small number and the integrated trajectory does not agree with the polynomial representation, either too few legs were used or the problem is ill-posed. Indications of insufficient legs are the presence of large discontinuities of the controls at the patch points and significant changes in the solution as the number of legs is increased. Typically, solutions which satisfy the equations of motion quite well require only 3 legs.

The accuracy with which a trajectory can be represented by polynomials is quite good. Previous studies[5, 8] indicate that trajectories can often be represented to accuracies which tax most numerical integrators.

SIMULATION DESCRIPTION

The equations of motion which were used correspond to a point mass vehicle in flight above a flat earth in still air with constant gravity. A cartesian coordinate system is used in which the aircraft dynamics can be expressed by

$$\mathbf{x}'' = (\mathbf{T}+\mathbf{L}+\mathbf{D})/m - \mathbf{g} \tag{9}$$

$$m' = \eta T_m s_{fc} \tag{10}$$

The controls employed are the power setting, η (constrained between 0 and 1) and the inertial attitude of the vehicle's longitudinal axis, $\mathbf{b}$. This vector can be resolved into components with an azimuth angle ϕ and an elevation angle θ.

$$\mathbf{b} = \begin{Bmatrix} \cos\theta\cos\phi \\ \cos\theta\sin\phi \\ \sin\theta \end{Bmatrix} \tag{11}$$

For the computation of the aerodynamic forces, it is assumed that $\sin\alpha = \alpha$ and that there is no sideslip. Lift and drag coefficients are obtained from the relationships

$$C_L = C_{L_\alpha}\sin\alpha \tag{12}$$

and

$$C_D = C_{D_0} + kC_L^2 + aC_L^4$$

The aerodynamic and propulsive forces are given by

$$\mathbf{T} = T_m \mathbf{b} \tag{13}$$

$$\mathbf{L} = \tfrac{1}{2}\rho S C_{L_\alpha}(\mathbf{b} \times \mathbf{v} \times \mathbf{v}) \tag{14}$$

$$\mathbf{D} = \tfrac{1}{2}\rho v S C_D \mathbf{v} \tag{15}$$

The dynamic system described by equations (9)–(15) can be applied to any lifting, thrusting vehicle. The quantities needed to define a particular vehicle are C_{L_α}, C_{D_0}, k, and a, which are represented as tabular functions of Mach number, and T_m and s_{fc}, which are tabular functions of Mach number and altitude. Accurate values for these parameters are generated by a high-fidelity ramjet simulation program which also constructs the required tables. Interpolation of these tables is accomplished by means of quintic splines in order to provide continuous first and second derivatives. Maximum thrust and specific fuel consumption are normalized by pressure ratio and temperature ratio, respectively, prior to interpolation to reduce the range of values encountered by the splines. Values of the NACA 1962 Standard Atmosphere are computed at a number of discrete points and interpolated in the same manner. Inequality constraints on altitude and lift coefficient can be imposed, although these were not required for every problem.

NUMERICAL RESULTS

Three types of trajectory optimization problems for a conventional air-to-air, liquid fuel, ramjet-powered missile were analysed. The problems consisted of minimum fuel-to-climb, minimum time-to-climb, and minimum time-to-intercept for both two- and three-dimensional intercepts. Trajectory profiles for each problem are illustrated.

Typical air-to-air, ramjet-powered missiles are accelerated from a subsonic velocity to a velocity between Mach 2 and Mach 3 by a rocket booster. All presented results reflect trajectory optimizations on only the ramjet-powered phase of the flight. The trajectory during the boost phase was assumed to be a constant 5 g pull-up after a horizontal launch.

A cubic polynomial patched through the boundary conditions was used as an initial trajectory for all the cases. The cubic was then used to initialize the parameter vector $\mathbf{z}$. All computations were performed on the Boeing CDC Cyber 175 computer.

Minimum fuel-to-climb

The minimum fuel-to-climb problem is an often-studied problem with vehicles employing airbreathing engines. The initial conditions for this problem, as well as most other problems presented in this paper, are an altitude of 31,600 ft, 2·98 Mach number, and a flight path angle of 18·5°. These conditions are typical following a rocket boost from an altitude of 30,000 ft and a Mach number of 0·8 with a pull-up manoeuvre.

The final conditions imposed for this problem were final altitude of 70,000 ft, 0° flight path angle, and a Mach number of 4·0. No final mass constraint was imposed. The optimum trajectory, as derived by CTOP, is a parabolic type of trajectory as shown in Figure 1.

In fact, the path almost describes a circular arc, as shown in Figure 2. This Figure illustrates that a simple circular arc climb is a reasonable trajectory to use where a trajectory close to the minimum fuel-to-climb is desired, but the absolute optimum trajectory is not required.

Throughout the climb, the missile used the maximum allowable fuel flow consistent with a 5 per cent supercritical margin on inlet pressure recovery. Figures 3 and 4 show the resulting thrust and Mach number profiles, respectively. As shown, the increase in altitude (hence decrease in atmospheric pressure and density) causes the maximum thrust to decrease. Mach number increases

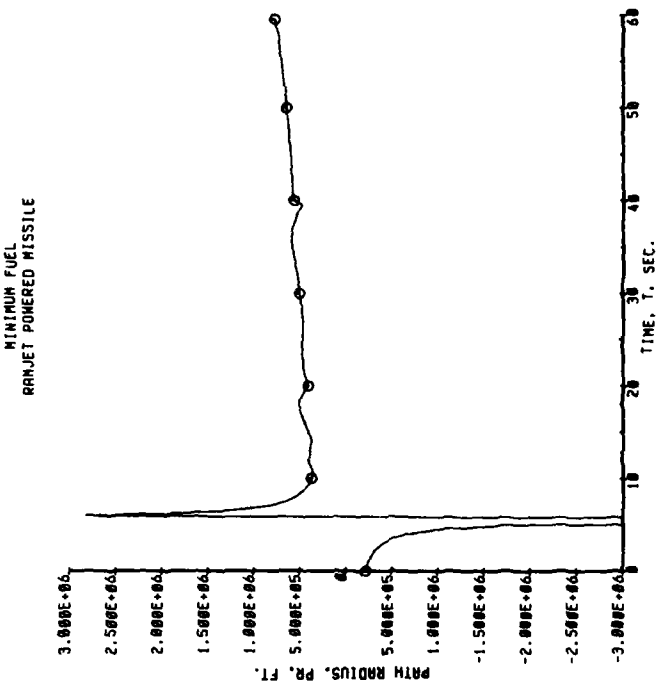

Figure 2. Minimum fuel-to-climb path radius

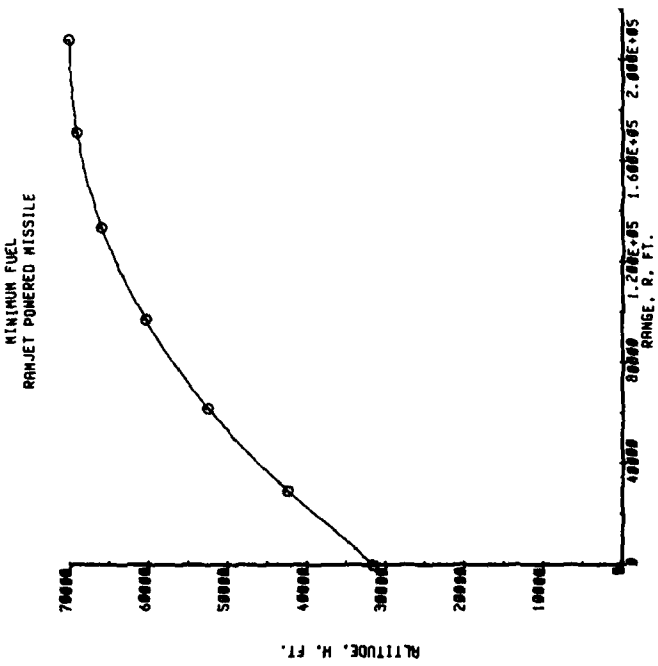

Figure 1. Minimum fuel-to-climb trajectory

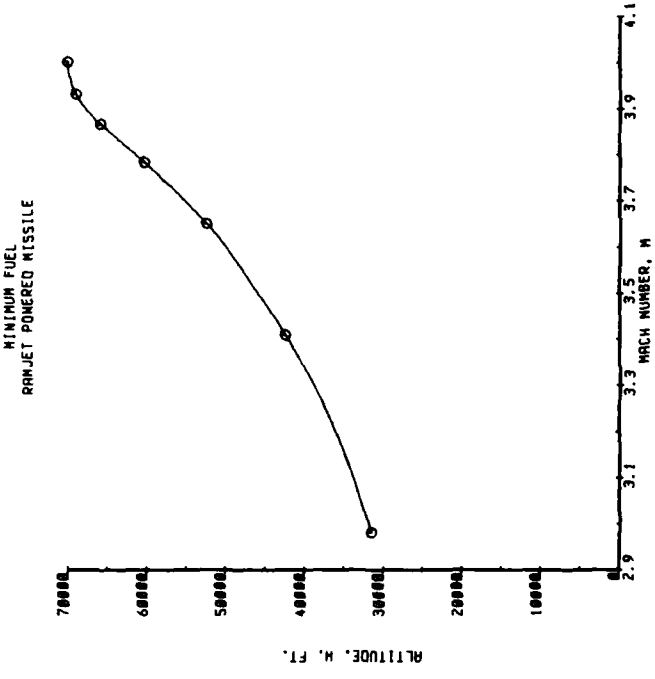

Figure 4. Minimum fuel-to-climb altitude–Mach relation

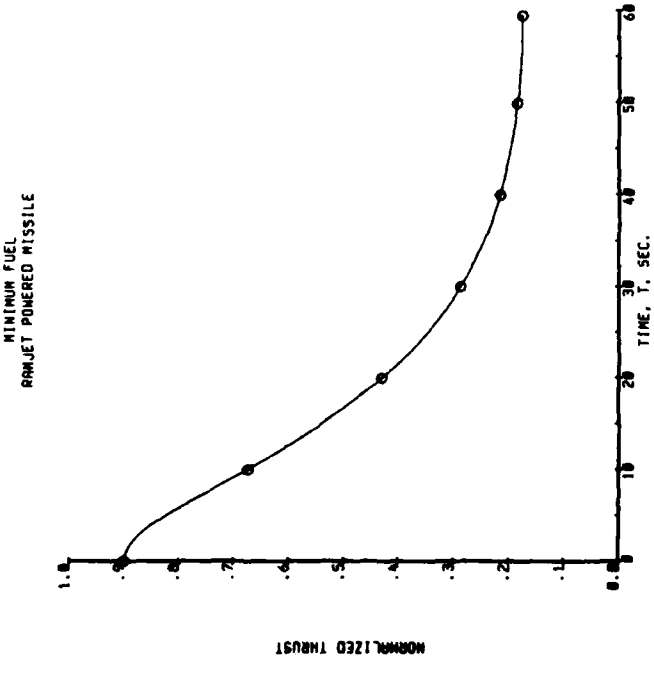

Figure 3. Minimum fuel-to-climb thrust profile

with altitude, and the rate of increase in Mach number is greater at the beginning of the trajectory than at the end. This solution, generated by CTOP, was checked with a detailed ramjet flight simulation program. Near identical agreement was obtained between the two computer programs.

Minimum time-to-climb

A minimum time-to-climb problem was solved to compare with the minimum fuel-to-climb problem and to investigate the characteristics of a trajectory which has implications in an air-to-air intercept scenario. The initial and final conditions for the problem were the same as those used in the minimum fuel-to-climb problem. The optimum trajectory is compared with that of the minimum fuel-to-climb in Figure 5.

As shown, the minimum time-to-climb trajectory has a reflex curve at the beginning. A similar flight path for a supersonic airplane was derived by Bryson for minimum time-to-climb.[9, 10] The dive before the climb was described as a trade between potential and kinetic energy in the Earth's gravitational field to assist with acceleration through the high-drag region near Mach 1. The ramjet flies at Mach numbers greater than Mach 2·96. Hence, there is no comparable 'high-drag region' for the ramjet to accelerate through. The ramjet dives to take advantage of its greater thrust capability at lower altitudes. The thrust versus time profile of the minimum time-to-climb is compared to that of the minimum fuel-to-climb trajectory in Figure 6.

The thrust, and hence acceration, for the minimum time-to-climb trajectory is greater because of the increased air pressure and density at lower altitudes. The resulting altitude and Mach number relations from the two trajectories are shown in Figure 7. Unlike the previous problem, the missile flies at the lower altitudes to increase Mach number before climbing. The minimum time-to-climb was 28 per cent less than that for the minimum fuel-to-climb problem, but it required 38 per cent more fuel.

A second minimum time-to-climb problem was analysed with an initial altitude of 41,400 ft, Mach number of 3·26, and flight path angle of 15·3°. Even with the same final conditions as the previous problems, the time required to climb was slightly longer than for the previous problem. One's first impression would be that the greater initial altitude would result in less time-to-climb, when in actuality, the time is longer. Figure 8 compares the two minimum time-to-climb trajectories. Both trajectories have a reflex curve at the beginning. Figure 9 shows that the thrust levels for the previous problem are higher since it was at a lower altitude. As a result, the previous minimum time-to-climb trajectory accelerated faster as shown in Figure 10. The missile that began at the lower altitude was able to increase its Mach number faster, and this more than offset the longer flight path.

Minimum time to intercept

Two-dimensional intercepts. Of particular interest in an air-to-air intercept scenario is the minimum time to intercept a target. Three two-dimensional (in vertical plane) and two three-dimensional intercept problems were evaluated. All problems used the same initial conditions as the minimum fuel-to-climb problem. The final conditions were to intercept the target in minimum time. No constraints were placed on the final flight path angle and velocity.

The three two-dimensional trajectories were against a non-manoeuvering target at 50,000 ft, travelling at Mach 2·5 away from the missile, with initial range separation distances of 50,000, 100,000, and 150,000 ft (8·2, 16·4, and 24·7 n mi). The first two problems were first solved with no constraint on the final weight of the missile. The resulting trajectories are shown in Figure 11.

These trajectories have the characteristic reflex at the beginning of the trajectory which also occurred in the minimum time-to-climb problems. The fuel flow rate was at its maximum allowable limit throughout the flights. However, the resulting final weights of the missiles were 7 per cent and

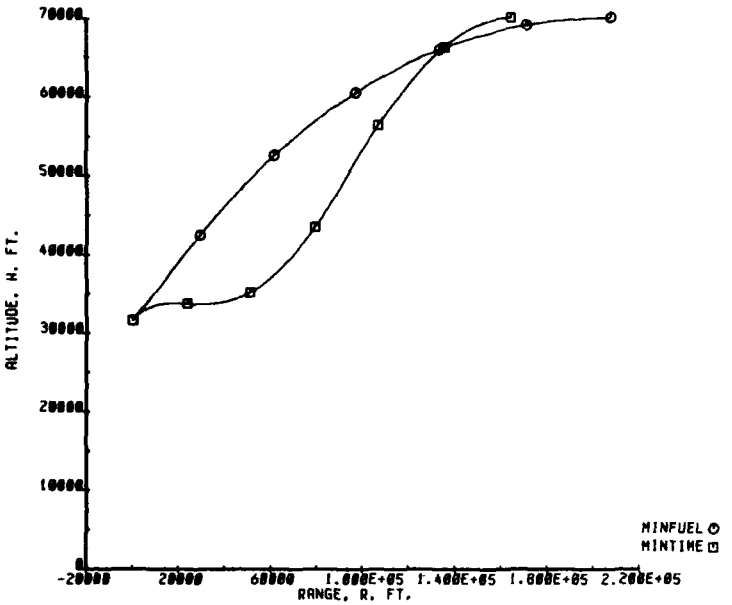

Figure 5. Comparison of climbing trajectories

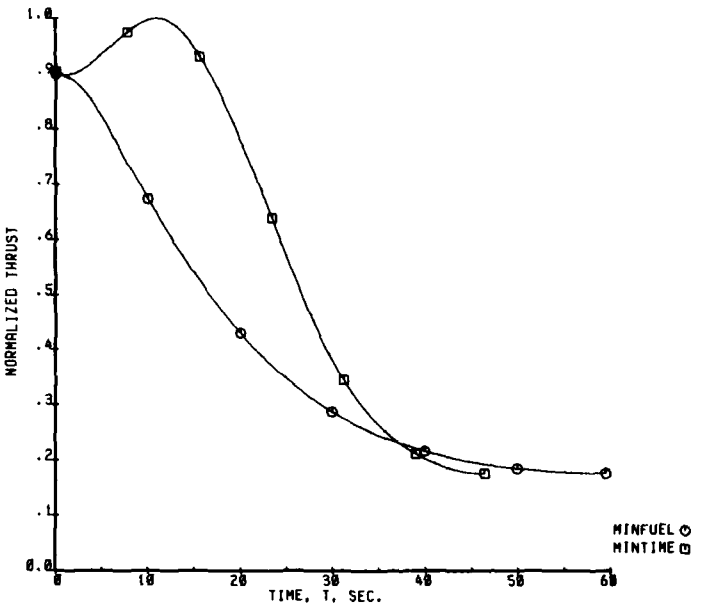

Figure 6. Comparison of thrust profiles

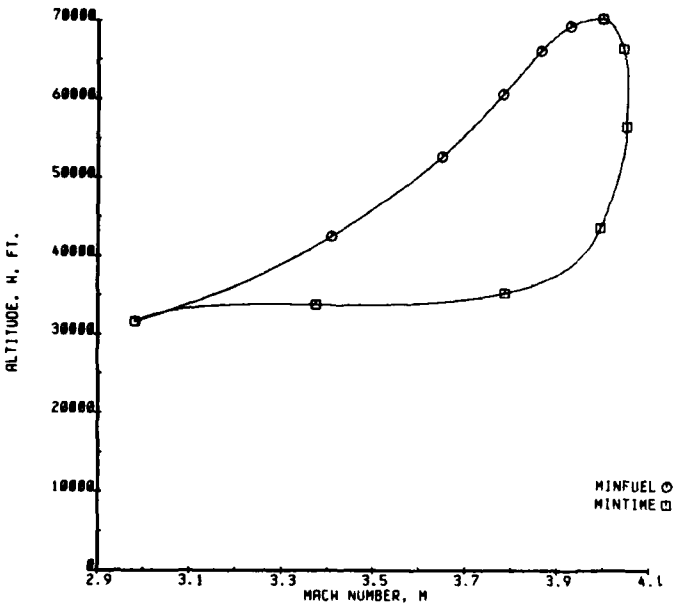

Figure 7. Comparison of altitude–Mach relation

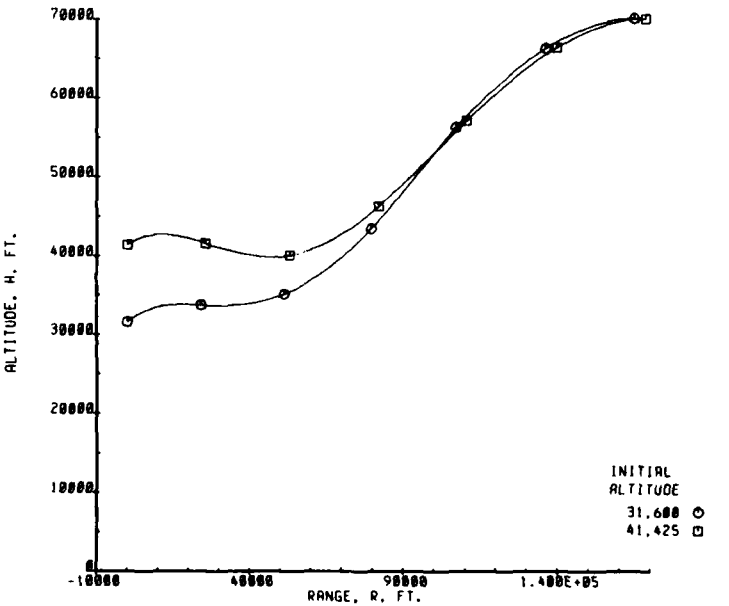

Figure 8. Comparison of minimum time-to-climb trajectories

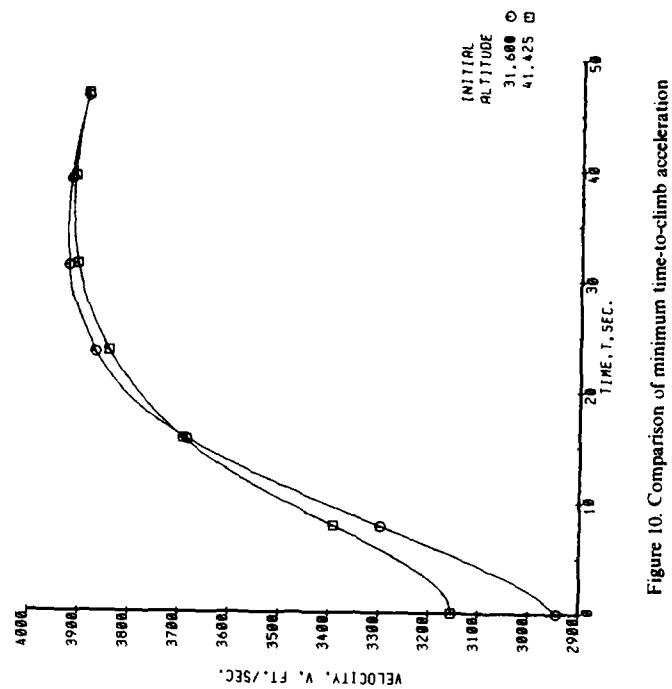

Figure 10. Comparison of minimum time-to-climb acceleration

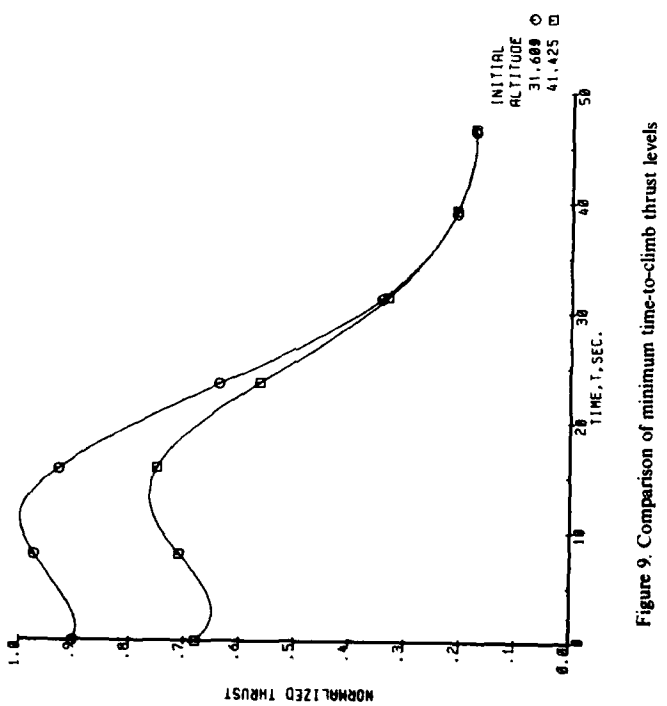

Figure 9. Comparison of minimum time-to-climb thrust levels

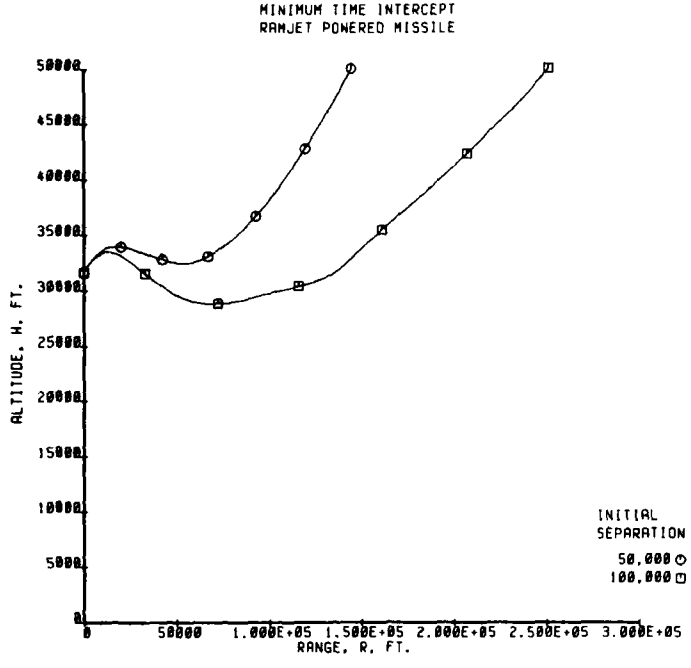

Figure 11. Comparison of intercept trajectories (no final weight constraint)

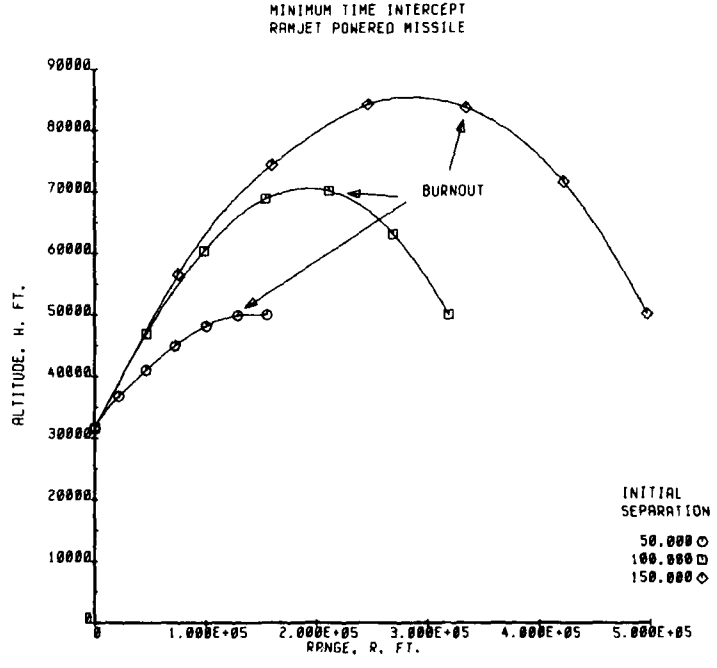

Figure 12. Comparison of intercept trajectories (with weight constraint)

28 per cent less than the estimated empty weight. These two problems, as well as a third problem which had the initial separation distance of 150,000 ft, were analysed with a constraint on the final weight. The resulting trajectories are shown in Figure 12.

The trajectories with the final weight constraint are significantly different from the other minimum-time trajectories. Instead of having a reflex type of trajectory, they are a lofted type of trajectory. A second difference is that the fuel flow is terminated soon after achieving the maximum altitude.

Three-dimensional intercepts. The two three-dimensional minimum time-to-intercept problems are similar to the two-dimensional problem with the initial range separation distance of 100,000 ft. In one case, the target is flying at a right angle to the initial missile path. In the other case, the target is flying at a 45° angle toward the missile, as illustrated in Figure 13. The three-dimensional problems had a final weight constraint.

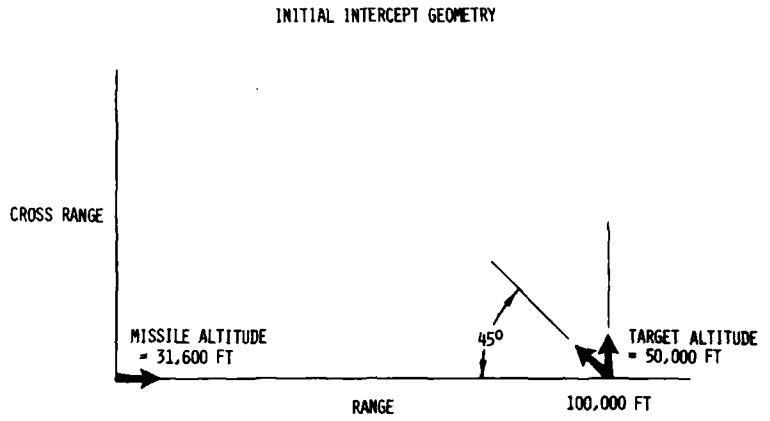

Figure 13. Initial geometry

The optimum trajectory for the case where the target is travelling 90° to the path of the missile is shown in Figure 14. Unlike the other intercept trajectories, this one shows a climb at almost a constant angle. Similar to the two-dimensional trajectories, the fuel flow is terminated near the end of the trajectory.

Figure 15 shows the trajectory for the case in which the target is flying at a 45° angle towards the path of the missile. Like the minimum time-to-climb problems, the trajectory shows a reflex path at its beginning. The fuel flow rate was at its maximum allowable rate throughout the trajectory. The reason for the difference in trajectory and fuel control characteristics between this and the other intercept trajectories with a constraint on the final weight is due to the shorter distance and lower flight time in this problem. The missile could fly at full throttle the entire mission and match the weight constraint.

APPENDIX: NOMENCLATURE

A coefficient matrix

B coefficient for ramp function, equation (5)

a quartic drag coefficient

b body attitude vector

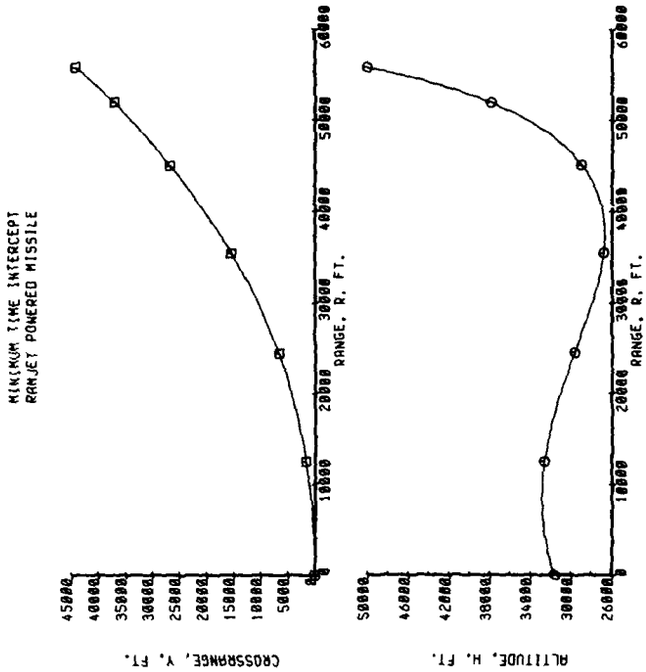

Figure 15. Trajectory for 45° target path

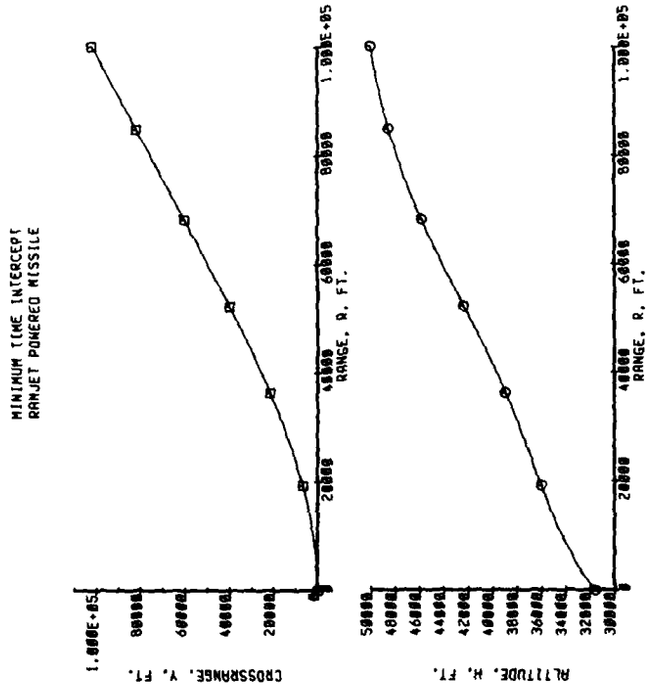

Figure 14. Trajectory for 90° target path

C_D drag coefficient
C_{D_0} zero lift drag coefficient
C_L lift coefficient
C_{L_α} lift curve slope
D drag
f second-order differential equation function
g first-order differential equation function; acceleration due to gravity
g acceleration due to gravity
h inequality constraint
J performance index
k induced drag coefficient
L lift
m mass
P^* augmented performance index
S planform area
s_{fc} specific fuel consumption
T thrust
T_m maximum thrust
t time
u control
V ramp function
v velocity
W weighting matrix
w parameter values
x state variable governed by a second-order differential equation
y state variable governed by a first-order differential equation
z optimization parameters
α angle of attack
ε penalty function weighting factor
η power setting
θ elevation angle
ρ atmospheric density
Φ performance function of the final conditions
ϕ azimuth angle

superscripts

(') differentiation with respect to time

subscripts

f at the final time

i at the initial time

REFERENCES

1. Fink, L. E. and B. M. Dunn, 'An automated procedure for integrated simulation and optimization of ramjet missile sizing and performance', *1979 JANNAF Propulsion Meeting*, **5**, 209–222 (1979).
2. Dunn, B. M. and L. E. Fink, 'Performance optimization study of a solid fuel ramjet powered missile for an air-to-air mission', *1979 JANNAF Propulsion Meeting*, **5**, 223–248 (1979).
3. Johnson, Forrester T., 'Approximate finite thrust trajectory optimization', AIAA Journal, **7**, 993–997 (1969).
4. Hahn, D. W., F. T. Johnson and B. F. Itzen, 'Interplanetary low-thrust mission design via Chebychev optimization methods', *Proceeding of the Eighth International Symposium on Space Technology and Sciences*, Tokyo (1969).
5. Hargraves, C. R., F. T. Johnson, S. W. Paris and I. H. Rettie, 'Numerical computation of optimal evasive maneuvers for a realistically modeled airplane pursued by a missile with proportional guidance', *AIAA paper 79-1624, AIAA Atmospheric Flight Mechanics Conference*, Boulder, Colorado, 6–8 August (1979).
6. Balakrishnan, A. V., 'On a new computing technique in optimal control', *SIAM Journal on Control*, **6**, 143–173 (1968).
7. Faddeeva, V. N., *Computational Methods of Linear Algebra*, Dover, New York, pp. 81–85, 1959.
8. Nacozy, P. E. and T. Feagin, 'Approximations of interplanetary trajectories by Chebychev series', *AIAA Journal*, **10**, 243–244 (1972).
9. Ashley, H., *Engineering Analysis of Flight Vehicles*, Addison-Wesley, Massachusetts, p. 369, 1974.
10. Bryson, A. E., 'Application of optimal control theory in aerospace engineering', *Journal of Spacecraft and Rockets*, **4**, 545–552 (1967).